DOI: 10.1002/chem.201201634

A Carborane-Derivative "Click" Reaction under Heterogeneous Conditions for the Synthesis of a Promising Lipophilic MRI/GdBNCT Agent**

Antonio Toppino,[a] Maria Elena Bova,[a] Simonetta Geninatti Crich,[a] Diego Alberti,[a] Eliano Diana,[a] Alessandro Barge,[b] Silvio Aime,[a] Paolo Venturello,[a] and Annamaria Deagostino*[a]

Abstract: In this study, the Huisgen reaction has been used to functionalise a carborane cage with a lipophilic moiety and a 1,4,7,10-tetraazacyclododecane-1,4,7,10-tetraacetic acid (DOTA) ligand to obtain a new Gd boron neutron-capture therapy (BNCT)/magnetic resonance imaging (MRI) agent. The introduction of the triazole units has been accomplished under both heterogeneous conditions, by the use of a Cu-supported ionic-liquid catalyst, and homogeneous conditions. The ability of the Gd complex of the synthesised ligand to form stable adducts with low-density lipoproteins (LDLs) has been evaluated and then MRI has been performed on tumour melanoma cells incubated in the presence of a Gd-complex/LDL imaging probe. It has been concluded that the high amount of intracellular boron necessary to perform BNCT can be reached even in the presence of a relatively low-boron-containing LDL concentration.

Keywords: carboranes · click chemistry · cycloaddition · heterogeneous catalysis · magnetic resonance imaging

Introduction

Boron neutron-capture therapy (BNCT) is a binary radiation therapy for the treatment of cancer that is based on the capture of thermal neutrons by ^{10}B nuclei that have been selectively delivered to tumour cells. The neutron-capture event results in the formation of excited ^{11}B nuclei that undergo fission to yield highly energetic $^{4}He^{2+}$ and $^{7}Li^{3+}$ ions. Cell death is triggered by the release of these charged particles, which create ionisation tracks along their trajectories, thereby resulting in cellular damage. It has been estimated that approximately 10–30 μg of boron per gram of tumour mass is needed to attain an acceptable therapeutic advantage.[1–3] Thus an important aspect relies on the possibility of delivering high payloads of ^{10}B at the target sites. Although clinical exploitation of the BNCT strategy is currently being carried out with lower-molecular-weight boron delivery agents, it is easy to consider polynuclear boron derivatives as potential candidates for BNCT applications. In fact, several readily functionalised carboranes have been employed to construct boron delivery vehicles for BNCT, because of their high content of boron and their stability in vivo.[4–7]

Click chemistry is a modular approach to organic synthesis that uses the most practical and reliable chemical transformations to construct target molecules.[8–10] In particular, the Cu^{I}-catalysed formation of the 1,2,3-triazolic ring, starting from azides and terminal alkynes, represents a powerful linking reaction owing to its high degree of dependability, complete specificity and biocompatibility of the reactants. Moreover, the triazolic moiety does not represent an inert linker and plays an active role since it readily associates with biological targets through hydrogen-bonding and dipole interactions. In recent years, there has been a significant interest in developing click reactions that do not require any metal catalyst yet they exhibit all the beneficial properties of the copper-catalysed azide–alkyne click reaction.[11]

The synthesis of a new dual agent for applications in magnetic resonance imaging (MRI)/BNCT has been recently developed in our laboratory, whereby a carborane unit is linked to a lipophilic chain and to a Gd–DOTA (DOTA = 1,4,7,10-tetraazacyclododecane-1,4,7,10-tetraacetic acid) complex through amidic bonds (AT101; Figure 1).[12]

According to the synthetic design, the lipophilic probe AT101 binds to low-density lipoproteins (LDLs) and accumulates at tumour cells characterised by an up-regulation of LDL transporters. The exploitation of LDL as biological vectors was indeed the key to obtaining a high concentration of B atoms per gram at the tumour cells together with a

[a] Dr. A. Toppino, M. E. Bova, Dr. S. Geninatti Crich, Dr. D. Alberti, Prof. E. Diana, Prof. S. Aime, Prof. P. Venturello, Dr. A. Deagostino
Dipartimento di Chimica
Università degli Studi di Torino
Via Pietro Giuria, 7, 10125 Torino (Italy)
Fax: (+39) 0116707642
E-mail: annamaria.deagostino@unito.it

[b] Dr. A. Barge
Dipartimento di Scienza e Tecnologia del Farmaco
Università degli Studi di Torino, Via Pietro Giuria, 9
10125 Torino (Italy)

[**] MRI = magnetic resonance imaging; BNCT = boron neutron-capture therapy.

Supporting information for this article is available on the WWW under http://dx.doi.org/10.1002/chem.201201634.

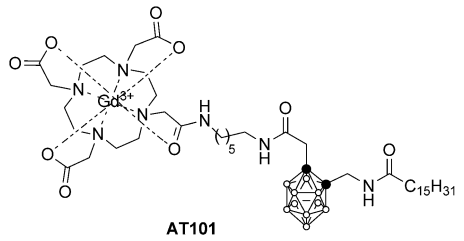

Figure 1. AT101: Gd^{III}--*C*-(*N*-DOTAMA-C_6-carbamoylmethyl)-*C*′-palmitamidomethyl-*o*-carborane complex.

good specificity for tumour cells. In vivo MR images acquisition showed that the amount of B taken up in the tumour region was above the threshold for a successful NCT treatment. After neutron irradiation, the treated mouse group showed a markedly lower tumour growth with respect to the control group.[13]

With the purpose of simplifying the synthetic procedure but maintaining, and possibly improving, the favourable properties of AT101, we designed a new structure that contained a triazole linker instead of the amidic function. Therefore we were interested in seeing how the chemical features of the five-membered ring could affect the biological behaviour of the desired dual agent. The 1,2,3-triazole function is a rigid linking unit that can mimic the atom placement and the electronic properties of the peptide bond, thereby avoiding the problem associated with the hydrolytic cleavage of the latter. Moreover, alkyne and azide are convenient and stable starting materials that can be introduced independently and do not react with common organic reagents or functional groups in biomolecules.[14] In addition, Huisgen cyclisation simplifies the synthesis of the substituted carborane, which has to be linked to the DOTA moiety. Although several authors have recently reported the synthesis of the Gd–DOTA complex by resorting to Huisgen cycloaddition,[15–21] this synthetic strategy might present some problems because of the high affinity of DOTA towards various metals. In particular, when comparing the equilibrium constant ($\log K_{ML}$) of DOTA–Gd and DOTA–Cu complexes (24.7 and 22.7, respectively),[22–24] one might surmise that Gd complexation could be partially or totally hampered by the presence of large amounts of Cu^{2+} ions. Since residual Cu coupling was observed in ESI mass spectral analysis, many efforts have been recently made toward developing "copper-free" methodologies for the introduction of the triazole scaffold in Gd–DOTA complexes by the use of very active alkynes.[25,26] Moreover, methods that exploit, for example, Na_2S to precipitate Cu^{II} at the end of the reaction or by means of the thio acid/sulfonyl azide amidation have also been reported.[20]

Even though innovative methodologies that utilise immobilised Cu catalysts have been recently described, in some cases copper hydroxide is used[27,28] or basic conditions are necessary.[29,30] These procedures could not be utilised in the case of carboranes that might be converted to *nido* carboranes in basic medium. Consequently, we focused our attention on the method proposed by Hagiwara et al.[31] which uses the Cu-supported ionic-liquid catalyst (SILC). Cuprous bromide is immobilised in the pores of amorphous silica gel with the aid of an ionic liquid (1-butyl-3-methylimidazolium hexafluorophosphate, or [bmim]PF_6).

Although some examples of Huisgen cyclisation applied to carboranes have been previously described,[32–35] to the best of our knowledge, the results reported here represent the first example of a Huisgen cyclisation that exploits an immobilised Cu^{I} catalyst in carborane chemistry. Then the ability of the Gd complex of the synthesised ligand to form stable adducts with LDLs was evaluated and an MRI assessment was carried out on tumour melanoma cells incubated in the presence of the Gd/B dual probe.

Results and Discussion

The synthetic approach started from benzyl but-3-ynyl ether (**2**), which was treated with paraformaldehyde to afford 5-benzyloxypent-2-ynol (**3**), as previously reported (Scheme 1).[12,36] The corresponding disubstituted *ortho*-carborane (**4**) was then obtained by reaction of the unprotected alcohol **3** with decaborane in a mixture of toluene/(bmim)Cl at 90 °C. The reaction was carried out in the presence of a slight excess amount of alkyne (1.5 equiv). The product was isolated with a respectable yield after purification. The peak at 2585 cm^{-1} in the IR spectrum of **4** clearly indicated the presence of the carborane cage, and moreover, the success of the reaction was also confirmed by the detection of the characteristic boron isotopic distribution in the ESI mass spectrum (*m*/*z* 309 $[M+H]^+$).

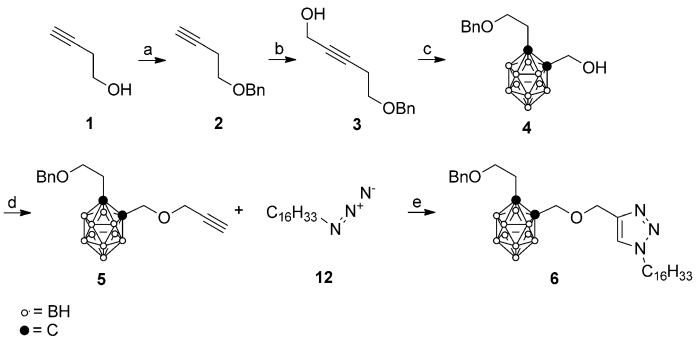

Scheme 1. Synthesis of *o*-carborane **6**. Reaction conditions and yields: a) BnBr, NaH, THF, RT (90%); b) BuLi, $(CH_2O)_n$, anhydrous THF, −20 °C→RT (65%); c) $B_{10}H_{14}$, $(bmim)^+Cl^-$, anhydrous toluene, 90 °C (44%); d) NaH, anhydrous THF, 0 °C→RT, then propargyl bromide, reflux overnight (85%); e) THF/H_2O 50:50, $Cu(OAc)_2$/$Na(C_6H_7O_6)$ 50:50 or EtOH/H_2O 50:50 (4 mL) and Cu–SILC (300 mg)/**6** (0.5 mmol).

The reaction between *C*-(2-benzyloxy)ethyl-*C*′-hydroxymethyl-*o*-carborane (**4**) and propargyl bromide afforded *C*-(2-benzyloxy)ethyl-*C*′-prop-2-ynyloxy-*o*-carborane (**5**) in good yields. The presence of the triple carbon–carbon bond was assessed by the appearance in the ^1H NMR spectrum of

intermediate **5** of the triplet centred at $\delta = 2.39$ ppm, attributable to the propargylic proton, and by the signals centred at $\delta = 73.0$ and 77.8 ppm in the ^{13}C NMR spectrum. The crude product was directly used for the subsequent Huisgen cyclisation reaction. The immobilisation of the copper catalyst on the functionalised silica gel was checked by vibrational spectroscopy before the Huisgen cyclisation was performed. The FT-Raman spectra of mercaptopropyl silica gel, of [bmim]PF_6 and of Cu–SILC have been compared. The spectrum of Cu–SILC appears by the superposition of the spectral features of [bmim]PF_6 and of mercaptopropyl modes, except for the intensity of the ν(S–H) mode at 2582 cm^{-1}, which shows an evident decrease in the Cu–SILC spectrum and is attributable to the formation of Cu–S bonds. In the stretching region of the Cu–S modes (250–450 cm^{-1}) some chain bending modes of [bmim]PF_6 units[37] are also present and this makes it difficult to provide a clear assignment of ν(Cu–S), which in our spectra is tentatively attributed to the medium-weak band at 413 cm^{-1} (see the Supporting Information). The Cu–SILC-catalysed reaction was accomplished in a 1:1 mixture of EtOH/H_2O in which the catalyst (300 mg of functionalised SiO_2/0.5 mmol of alkyne) was suspended with alkyne **5** and palmitylazide (**12**) according to the procedure described in the original paper of Hagiwara et al.[31] Afterwards the Huisgen cyclisation was optimised by changing the reaction temperature and the stoichiometric ratio between the reagents. To compare yields and results with those obtained in the Cu–SILC-catalysed process, the reaction was also carried out by using a stoichiometric amount of $Cu(OAc)_2$ and sodium ascorbate as the reducing agent. The Huisgen cyclisation reaction conditions in the latter case were optimised on a model system by using a mono-substituted *ortho* carborane. The reactions carried out in the presence of catalytic amounts of $Cu(OAc)_2$ afforded the desired product in low yields. The results are reported in Table 1. The yields obtained in the Cu–SILC-catalysed cyclisation were lower than those obtained using the homogeneous catalysis (Table 1, entry 1). This finding was not surprising if we consider that in the latter case a stoichiometric amount of catalyst was used. In the case of Cu–SILC-catalysed reactions, the temperature strongly affected the cyclisation rate, in fact when the reaction was carried out at 60 °C (Table 1, entry 3) the reactants turned into *C*-[1-hexadecyl-(1*H*-1,2,3-triazol-4-yl)-*C*′-2-hydroxyethyl-*o*-carborane (**6**) in 16 h. The same reaction carried out at RT (Table 1, entry 2) and at 40 °C (Table 1, entry 5) needed 7 days and 40 h, respectively, to finish. Yields were neither affected by increasing the reaction temperature nor by modifying the ratio between azide **12** and alkyne **5**.

Table 1. Huisgen reaction between *o*-carborane **5** and hexadecyl azide (**12**).

Entry	Catalyst	No. equiv alkyne/azide	*T* [°C]	*t* [h]	Yield [%][a]
1	$Cu(OAc)_2$/Na ascorbate[b]	1	RT	16	53
2	Cu–SILC[c]	1	RT	168	40
3	Cu–SILC[c]	1	60	16	36
4	Cu–SILC[c]	2	40	40	35
5	Cu–SILC[c]	1	40	40	35

[a] Isolated products, purified by column chromatography. [b] Reactions conditions: THF/H_2O 50:50, $Cu(OAc)_2$/$Na(C_6H_7O_6)$ 50:50. [c] Reactions conditions: EtOH/H_2O 50:50 (4 mL) and Cu–SILC (300 mg)/**6** (0.5 mmol).

Overall, the yields might be considered reasonable in light of the generally low reactivity of carboranes. Both the reaction catalysed by Cu–SILC and by $Cu(OAc)_2$ afforded only the less hindered regioisomer, as confirmed by the signal at $\delta = 7.51$ ppm in the ^1H NMR spectrum that corresponds to the C*H* group of the triazole ring. ^{13}C NMR spectroscopy showed two peaks at $\delta = 122.5$ and 143.1 ppm, which are attributable to the triazolic CH and quaternary C, respectively.

The functionalised carborane **6** was then deprotected by Pd/C hydrogenation to afford alcohol **7**, which was treated with propargyl bromide to give derivative **8** in good yields (Scheme 2). Compound **8** is the desired precursor for the Huisgen cyclisation with the DOTAMA-C_6-azide **15**.

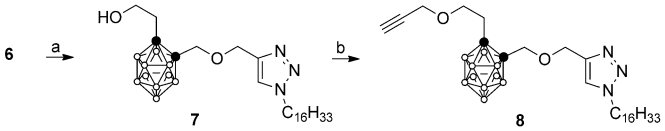

Scheme 2. Synthesis of *o*-carborane **8**. Reaction conditions and yields: a) 20% Pd/C, H_2 atmospheric, CH_2Cl_2/MeOH, RT (82%); b) NaH, anhydrous THF, 0 °C→RT, then propargyl bromide, reflux overnight (76%).

The presence of the triple carbon–carbon bond was assessed by the appearance of the multiplet at $\delta = 2.48$ ppm in the ^1H NMR spectrum, and by the two signals at $\delta = 74.91$ and 77.43 ppm in the ^{13}C NMR spectrum, which were assigned to the quaternary C and CH of the alkynic portion, respectively.

Compound **15** was obtained by starting from the corresponding alcohol DOTAMA-C_6-OH **13**,[38] which was previously transformed into the analogous mesylate **14** (Scheme 3). The formation of mesylate **14** and the subsequent conversion into azide **15** was confirmed by the corresponding ESI mass spectra in which the *m*/*z* 773 and 720 [M^++Na] peaks were detected. Moreover, in the ^1H NMR spectra of the DOTA-C_6 derivatives **13** and **14**, the disappearance of the signal centred at $\delta = 3.62$ ppm, relevant to the protons of the CH_2 bonded to the OH group, and the appearance of a new signal at $\delta = 4.15$ ppm that was attributable to the corresponding CH_2 group in mesylate **14** were meaningful. In the ^{13}C NMR spectrum the signal of the above-mentioned CH_2 group moved from $\delta = 61.80$ ppm in alcohol **13** to $\delta = 70.00$ ppm in mesylate **14** and to $\delta =$ 55.2 ppm in azide **15**. The synthesis of *C*-[(DOTAMA-C_6-(1*H*-1,2,3-triazol-4-yl)]ethyloxy-*C*′-[1-hexadecyl(1*H*-1,2,3-triazol-4-yl)]-*o*-carborane (**9**) was accomplished by using the optimised procedures described for the Huisgen cyclisation

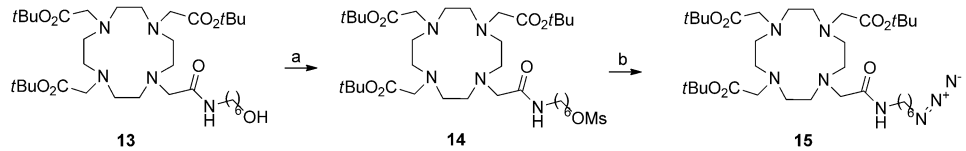

Scheme 3. Synthesis of DOTAMA-C_6-N_3 **15**: a) Et_3N, MsCl, anhydrous Et_2O, 0 °C→RT (77 %); b) NaN_3, anhydrous DMF, RT (64 %).

between *C*-(2-benzyloxy)ethyl-*C*′-prop-2-ynyloxy-*o*-carborane (**5**) and hexadecylazide (**12**). The Cu–SILC catalyst was suspended in a mixture of EtOH/H_2O 50:50 in which alkyne **8** and the azide **15** were dissolved and stirred overnight at 60 °C.

The disappearance of alkyne **8** was checked by TLC by looking for the disappearance of the spot attributable to **8**. After filtration and evaporation of the solvent the crude product was purified and the DOTA *tert*-butyl protecting groups were removed by using an excess amount of CF_3COOH at RT, as demonstrated by the disappearance of the *t*Bu signals in the NMR spectra of the product. Huisgen cyclisation was also carried out by using $Cu(OAc)_2$ in the presence of Na ascorbate to compare the yields with the ones of the Cu–SILC-catalysed process. The desired product **9** (Scheme 4) was obtained in 18 % yield when Cu–SILC

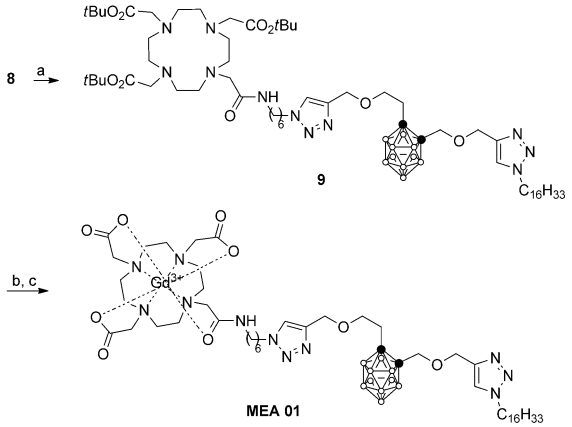

Scheme 4. Synthesis of Gd^{III}–MEA01. Reaction conditions and yields: a) DOTAMA-C_6N_3 **15**, THF/H_2O 50:50, $Cu(OAc)_2$/$Na(C_6H_7O_6)$ 1:1, RT (35 %) or EtOH/H_2O 50:50 (4 mL), Cu–SILC, 60 °C (18 %); b) CH_2Cl_2, CF_3COOH, RT (99 %), c) $GdCl_3$, H_2O, RT, pH 7.

was utilised, and in 35 % yield under homogeneous conditions. These low yields were not surprising because of the low reactivity of DOTA and carborane moieties. It should be stressed that in the former case a catalytic amount of immobilised recyclable Cu^+ was used, whereas in the latter the product was obtained by using a stoichiometric amount of catalyst. The mass spectrum of the final ligand **9** did not show any evidence of the Cu–MEA01 adduct, nor did it when Cu–SILC was used to introduce the triazole moiety when the Huisgen reactions were carried out under homogeneous conditions. Although, when using the Cu/B ratio determined by inductively coupled plasma (ICP)-MS, 14 and 35 % of Cu per ligand molecule was found in the two ligand solutions, respectively, the ligand titration with $GdCl_3$ in water at neutral pH followed by relaxometric measurements showed the equivalence point exactly at 1:1 ligand/metal concentration. This indicates the absence of interference by this small amount of Cu in the Gd complexation process.

Relaxometric characterisation of the Gd complex and LDL adduct preparation: The relaxivity (that is, the proton relaxation enhancement of water protons in the presence of the paramagnetic complex at 1 mM concentration) of MEA01 was measured at 21.5 MHz and 298 K and was found to be 16.8 $mM^{-1}s^{-1}$, which is in the typical range of slowly moving supramolecular adducts that involve the neutral Gd^{III}–DOTA monoamide moiety.

The various parameters affecting the observed proton relaxivity (r_{1p}) were assessed by analysing the dependence of the ^1H water relaxation rates as a function of the applied magnetic field ($1/T_1$ NMRD profile). The best fit of the data (Table 2) to the values calculated on the basis of the Solo-

Table 2. Best-fitting parameters obtained from the analysis of the NMRD profile by considering one inner-sphere water molecule ($q=1$), the protons of which are at an average metal distance of 3 Å.

	Δ^2 [$s^{-2}/10^{19}$]	τ_V [ps]	τ_R [ns]	τ_M [μs]
MEA01	1.2 ± 0.5	24 ± 3	66 ± 10	1 ± 0.3

mon–Bloembergen–Morgan equations (for the inner sphere contribution) and of Freed's equation (for the outer sphere contribution) indicates that the increase in relaxivity with respect to the parent Gd–DOTA complex is a result of significant lengthening of τ_r as a consequence of its self-assembling in water in micellar aggregates.

To pursue the formation of supramolecular adducts with LDLs, MEA01 micelles were disaggregated by using an excess amount of β-cyclodextrin (β-CD).[39] The transfer of the MEA01 units from the micelles to the supramolecular "host/guest" complex with β-CD was followed by measuring the relaxation rate of the solvent water protons. Then the stepwise addition of the β-CD/MEA01 adduct to the aqueous solution of LDL particles allowed the translocation of the amphiphilic molecules into the LDL particles to occur. This step was again assessed by measuring the changes in the relaxation enhancement of the solvent water protons (Figure 2). The analysis of the titration curve showed a reasonably high MEA01-to-LDL binding affinity ($K_a=(1.4\pm0.5)\times10^4\,M^{-1}$) and a number of binding sites on the surface of the LDLs equal to 300 ± 50. The dynamic light scattering (DLS) measurements indicated that the size of the formed LDL adducts ((21.8 ± 2) nm) was almost the same as that

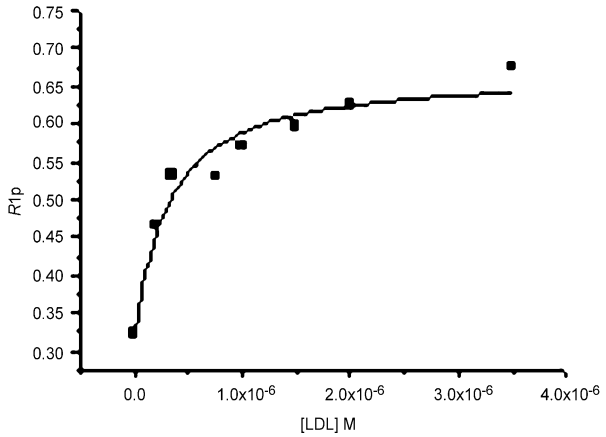

Figure 2. Titration of native LDL into the Gd/B/L–β-CD adduct. The samples were incubated for 2 h at 37 °C prior to the $R1$ measurements.

found in the native LDL particles ((22.5 ± 1) nm). This indicates the absence of any change in the overall protein structure upon the binding of B/Gd-containing units. On the basis of these results, one might conclude that, as far as the formation of inclusion complexes with LDL is concerned, the behaviour of MEA01 is very similar to what has previously been reported for AT101.

Cell uptake experiments: Using the method reported above, an MEA01/LDL adduct made up of 295 ± 15 Gd complex per protein was prepared by incubating LDL and β-CD/MEA01 340:1 for 2 h at 37 °C. After purification, about 76 % of the total protein was recovered as MEA01 adduct and the MEA01 loading efficiency into LDLs was 70 %. These values are similar to those obtained for the parent compound AT101.[40] The stability of MEA01/LDL in plasma was evaluated by measuring the relaxation rate of a 0.07 mM complex solution dissolved in human serum (seronorm) at 37 °C. The R_{1obsd} remained unchanged during the monitored period of 24 h. Furthermore, an increasing amount (0–150 mg mL^{-1}) of human albumin was added to a solution of MEA01 (0.07 mM) in phosphate buffer solution (PBS) without observing any increase of the paramagnetic contribution to the relaxation rate, thus excluding any interaction with this protein. We can conclude that the stability of the ME01/LDL adduct is high enough to prevent its dissociation when injected into the bloodstream.

Gd/B-loaded LDL particles were added to the B16 melanoma cell growth medium (previously incubated for 24 h with a lipoprotein deficient serum (LPDS) to increase LDL receptor expression).

Cellular labelling experiments proved that after 16 h of incubation in the presence of 10–50 μg mL^{-1} MEA01/LDL, the amount of internalised Gd was sufficient to generate hyperintense signals in MR images (Figure 3). The corresponding relaxation rates measured in the labelled cells showed saturation-like behaviour. Competition assays with free LDL were carried out to demonstrate that the uptake of the MEA01/LDL adduct from B16 cells involves LDLRs. After

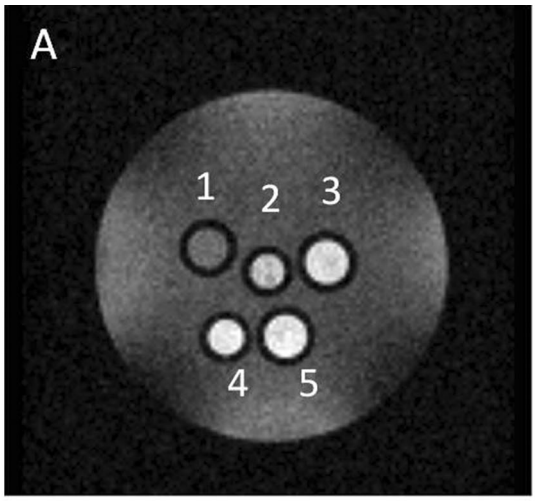

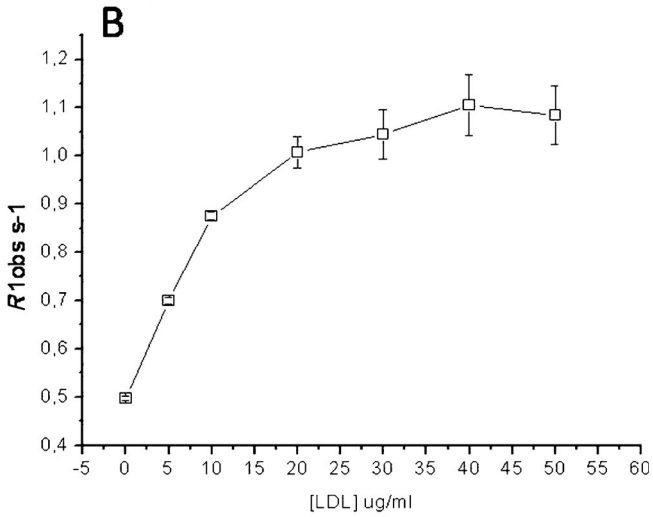

Figure 3. In vitro uptake experiments in cultured B16 cells. A) T_1-weighted spin–echo MR image of an agar phantom containing unlabelled cells (1) and cells incubated with 5, 10, 20 and 30 μg mL^{-1} of MEA01/LDL (2–4, respectively) for 16 h at 37 °C. B) Relaxation rates measured at 7 T in B16 cells incubated for 16 h at 37 °C with MEA01/LDL as a function of the concentration of LDL particles. The vertical lines indicate the standard deviations of the relaxation rates [s^{-1}].

16 h of cell incubation in the presence of the adduct (20 μg mL^{-1}), the uptake by B16 cells decreased by 65 % when the concentration of native LDL particles added to the culture medium was 150 μg mL^{-1}.

Table 3 shows the amount of Gd and B atoms internalised by B16, which was measured by ICP-MS after 16 h incubation in the presence of increasing amounts of MEA01/LDL (calculated under the assumption that 1 g of tissue contains 1×10^9 cells).

Table 3. Amount of Gd and B atoms internalised by B16 after 16 h incubation in the presence of increasing amounts of MEA01/LDL.

Entry	Adduct [μg per mL LDL]	Boron [ppm] (MEA01/LDL adduct)
1	10	16
2	20	22
3	30	28

We can conclude that, by using MEA01/LDL adduct, the minimum amount of intracellular boron necessary to perform BNCT (about 20 ppm) is reached at a relatively low boron-containing labelled LDL concentration.

Conclusion

In this study, it has been shown that the use of the Huisgen reaction greatly simplifies the synthesis of lipophilic GdBNCT/MRI agents. Moreover, a heterogeneous catalytic methodology has been applied to the insertion of carboranes for the first time. As a matter of fact, the proposed synthetic procedure allows the new ligand structure (MEA01) to be obtained in relatively good yields with significantly fewer steps than the previously reported AT101 system. In particular, the new synthetic strategy allows for the synthetic steps to be reduced from fourteen to nine and the overall yield to be improved from 3 to 8%, as evidenced in Table 4.

Table 4. Comparison of some properties of AT101 and MEA01.

	AT101	MEA01
synthetic steps	14	9
overall yield [%][a]	3	8.1
relaxivity [$mM^{-1}s^{-1}$]	17.3	16.8

[a] Isolated products, purified by column chromatography.

To take full advantage of the Gd–DOTA moiety as an MRI probe and allow the Gd–DOTA complex to be formed, the introduction of the triazoles as the linker between a carborane cage, a long alkylic chain and DOTA ligand, respectively, was previously accomplished by the use of Cu–SILC catalyst, whereby Cu^+ ions are immobilised on a silica gel matrix. The MRI/BNCT agent MEA01 was prepared by following a procedure that also exploits the homogeneous catalysis to compare the relaxivity properties and the biological behaviour in both cases. The complex obtained was fully characterised from the relaxometric point of view and, after disaggregation with β-cyclodextrin, MEA01/LDL adducts were prepared and the results showed a reasonably high MEA01-to-LDL binding affinity, very close to that of AT101 (Table 4). Finally, the MEA/01 adducts were tested in vitro on B16 melanoma cells and a suitable intracellular Gd/B concentration was detected after 24 h of incubation. This result is particularly useful in light of future in vivo applications in which higher concentrations of LDL adducts at the target site are usually difficult to reach. Furthermore, we can conclude that the substitution of amidic groups with triazolic rings does not significantly change the relaxometric properties of the Gd complex and its affinity for the biological carrier LDLs.

Experimental Section

General: Flasks and all equipment used for the generation and reaction of moisture-sensitive compounds were dried by using an electric heater under Ar. THF was distilled from benzophenone ketyl, anhydrous Et_2O was distilled from $LiAlH_4$ and anhydrous CH_2Cl_2 from CaH_2 prior to use. BuLi (1.6 M in hexanes) was obtained from Aldrich. $(Bmim)^+Cl^-$ was purchased from Solvent Innovation GmbH. Decaborane was bought from KATCHEM spol. sro. All commercially obtained reagents and solvents were used as received. Products were purified by preparative column chromatography on Macherey–Nagel silica gel for flash chromatography, 0.04–0.063 mm/230–400 mesh using mixtures of petroleum ether 40–60 (EP) and diethyl ether (EE) or $CHCl_2$ and MeOH as eluants. *o*-Carborane **9** was deprotected by following the procedure already reported.[12]

Reactions were monitored by TLC using silica gel on TLC-PET foils Fluka (2–25 mm, layer thickness 0.2 mm, medium pore diameter 60 Å). Carboranes and their derivatives were visualised on TLC plates by using a 5% $PdCl_2$ aqueous solution in HCl. ^1H NMR spectra were recorded at 200 MHz, ^{13}C NMR spectra at 50.2 MHz. Data were reported as follows: chemical shifts [ppm] from tetramethylsilane as internal standard, multiplicity (s = singlet, d = doublet, t = triplet, q = quartet, dd = double-doublet, m = multiplet, br = broad), coupling constants [Hz], integration and assignment. ^{13}C NMR spectra were measured with complete proton decoupling. Chemical shifts were reported [ppm] from the residual solvent as an internal standard. GC-MS spectra were obtained using a mass selective detector HP 5970 B instrument operating at an ionising voltage of 70 eV connected to an HP 5890 GC with a cross-linked methyl silicone capillary column (25 m × 0.2 mm × 0.33 mm film thickness). ESI-MS spectra were obtained using a Waters micromass ZQ spectrometer equipped with an ESI ion source. IR spectra were recorded using a Perkin–Elmer BX FTIR. The Cu−SILC catalyst was prepared by following the literature. Benzyl but-3-ynyl ether l (**2**) and 5-benzyloxypent-2-ynol (**3**) were synthesised as described in the literature and their spectroscopic data corresponded with those reported.[36]

The $1/T_1$ nuclear magnetic relaxation dispersion profiles of water protons were measured over a continuum of magnetic field strengths from 0.00024 to 2.4 T (which correspond to 0.01–80 MHz in proton Larmor frequency) using a fast field-cycling Stelar Spinmaster FFC relaxometer (from 0.01 to 20 MHz) and using a Stelar Spinmaster variable magnetic field instrument (from 20 to 80 MHz). The Gd, B and Cu content was determined by using inductively coupled plasma mass spectrometry (ICP-MS; element-2; Thermo-Finnigan, Rodano (MI), Italy). Sample digestion was performed with concentrated HNO_3 (70%, 2 mL) under microwave heating (Milestone MicroSYNTH Microwave labstation). Dynamic light-scattering measurements, which were made to determine the size of the micellar system, were performed using a Malvern Zetasizer SZ apparatus. A laser was used as the light source to illuminate the sample particles within the cell.

Procedure for the azide–alkyne cycloaddition in hetereogeneous and homogeneous conditions:

o-*Carborane* ***6***: Method A: *o*-Carborane **5** (0.72 mmol, 0.25 g) and palmitilazide **12** (0.72 mmol, 0.19 g) in a 25 mL round-bottomed flask were suspended in a solution of H_2O/MeOH (4 mL, 1:1) with Cu−SILC (450 mg) and stirred at 60 °C overnight under Ar. The solution was then filtered and the solvent was evaporated. The crude was purified by column chromatography (eluent: CH_2Cl_2/MeOH 99:1) to afford a pale yellow oil (0.18 g, 40%). Method B: *o*-Carborane **5** (1.50 mmol, 0.53 g) and palmitilazide **12** (1.50 mmol, 0.40 g) in a 50 mL round-bottomed flask were dissolved in H_2O/THF (10 mL, 50:50) and stirred overnight at RT in the presence of $Cu(OAc)_2$ (1.50 mmol, 0.30 g) and Na ascorbate (1.50 mmol, 0.30 g). The THF was then removed by evaporation and CH_2Cl_2 was added. The aqueous phase was then extracted twice with CH_2Cl_2 and the organic phases were washed with brine (2 × 10 mL). The crude was purified by column chromatography (eluent: CH_2Cl_2/MeOH 99:1) to afford a pale yellow oil (0.23 g, 53%). ^1H NMR (200 MHz, $CDCl_3$, Me_4Si): δ = 0.89 (br t, J = 8.3 Hz, 3H; CH_3), 1.26 (br s, 26H; $CH_3(CH_2)_{13}$), 1.87 (m, 2H; $CH_3(CH_2)_{12}CH_2$), 2.47 (t, J = 6.8 Hz, 2H; $PhCH_2OCH_2CH_2$), 3.59 (t,

J=6.8 Hz, 2H; $PhCH_2OCH_2CH_2$), 4.08 (s, 2H; $B_{10}H_{10}C_2CH_2O$), 4.29 (t, J=7.2 Hz, 2H; $(CH_2)_{13}CH_2CH_2N_3C_2$), 4.47 (s, 2H; $OCH_2N_3C_2$), 4.65 (s, 2H; $PhCH_2O$), 7.34 (m, 5H; $PhCH_2OCH_2CH_2$), 7.48 ppm (s, 1H; HN_3C_2); ^{13}C NMR (50.2 MHz, $CDCl_3$, Me_4Si): δ=14.0 (q), 22.5 (t), 26.3 (t), 28.8 (t), 29.2 (5×t), 29.4 (2×t), 29.5 (2×t), 30.1 (t), 31.8 (t), 34.6 (t), 50.2 (t), 64.5 (t), 68.2 (t), 69.7 (t), 73.0 (t), 75.5 (s), 76.8 (s), 122.3 (d), 127.5 (2×d), 127.7 (d), 128.3 (2×d), 137.4 (s), 143.4 ppm (s); IR (neat): $\tilde{\nu}_{max}$=2925, 2854, 2585, 1456, 1103 cm^{-1}; MS (ESI+): m/z: 614 $[M+H]^+$; elemental analysis calcd (%) for $C_{31}H_{59}B_{10}N_3O_2$: C 60.65, H 9.69, N 6.84; found C 60.68, H 9.67, N 6.85.

o-*Carborane* **7**: *o*-Carborane **6** (2.8 mmol, 0.17 g) in a 25 mL round-bottomed flask was dissolved in a solution of CH_2Cl_2/MeOH (15 mL, 50:50), then Pd/C was added (20% w/w, 34 mg), the solution was stirred at RT overnight under H_2 atmosphere. The solution was then filtered and the solvent was removed by evaporation. The crude was purified by column chromatography (eluent: CH_2Cl_2/MeOH 99:1) to afford a pale yellow oil (0.12 g, 82%). ^1H NMR (200 MHz, $CDCl_3$, Me_4Si): δ=0.90 (brt, J=6.6 Hz, 3H; CH_3), 1.25 (brs, 26H; $CH_3(CH_2)_{13}$), 1.91 (m, 2H; CH_3-$(CH_2)_{13}CH_2$), 2.42 (t, J=7.0 Hz, 2H; $HOCH_2CH_2$), 2.50 (brs, 1H; HO), 3.74 (t, J=7.2 Hz, 2H; $HOCH_2CH_2$), 4.12 (s, 2H; $B_{10}H_{10}C_2CH_2O$), 4.35 (t, J=7.2 Hz, 2H; $(CH_2)_{12}CH_2CH_2N_3C_2$), 4.66 (s, 2H; $HOCH_2N_3C_2$), 7.51 ppm (s, 1H; HN_3C_2); ^{13}C NMR (50.2 MHz, $CDCl_3$, Me_4Si): δ=13.9 (q), 22.5 (t), 26.3 (t), 28.8 (t), 29.1 (t), 29.2 (4×t), 29.3 (2×t), 29.5 (2×t), 30.0 (t), 31.7 (t), 37.1 (t), 50.4 (t), 60.5 (t), 64.0 (t), 70.0 (t), 75.4 (s), 77.1 (s), 122.7 (d), 143.0 ppm (s); IR (neat): $\tilde{\nu}_{max}$=3368, 2928, 2585, 1467, 1052 cm^{-1}; MS (ESI+): m/z: 524 $[M+H]^+$; elemental analysis calcd (%) for $C_{24}H_{53}B_{10}N_3O_2$: C 55.03, H 10.20, N 6.11; found: C 55.00, H 9.87, N 6.11.

o-*Carborane* ***8***: *o*-Carborane **7** (0.28 mmol, 0.15 g) in a 50 mL three-necked round-bottomed flask was dissolved in anhydrous THF (20 mL) and cooled to 0°C, then NaH (2.5 equiv, 0.7 mmol, 0.02 g) was slowly added. The reaction mixture was stirred at 0°C for 20 min and at RT for 1 h, then 80% propargyl bromide solution was added (5 equiv, 1.4 mmol, 0.13 mL). The reaction was stirred at reflux overnight and was then quenched with a saturated aqueous NH_4Cl and extracted with Et_2O (3×10 mL). The combined extracts were washed with brine (1×10 mL), dried and evaporated under reduced pressure. The crude was purified by column chromatography (eluent: EP/EE 99:1) to afford a pale yellow oil (0.12 g, 76%). ^1H NMR (200 MHz, $CDCl_3$, Me_4Si): δ=0.88 (brt, J=6.4 Hz, 3H; CH_3), 1.26 (brs, 26H; $CH_3(CH_2)_{13}$), 1.95 (m, 2H; CH_3-$(CH_2)_{12}CH_2$), 2.46 (m, 3H; $B_{10}H_{10}C_2CH_2CH_2O_2$, ≡CH), 3.61 (t, J=7.0 Hz, 2H; $B_{10}H_{10}C_2CH_2CH_2O$), 4.09 (s, 2H; $OCH_2B_{10}H_{10}$), 4.12 (d, J=2.4 Hz, 2H; $CH_2C{\equiv}CH$), 4.36 (t, J=7.2 Hz, 2H; $(CH_2)_{12}CH_2CH_2N_3C_2$), 4.70 (s, 2H; $OCH_2N_3C_2$), 7.27 ppm (s, 1H; HN_3C_2); ^{13}C NMR (50.2 MHz, $CDCl_3$, Me_4Si): δ=13.9 (q), 22.4 (t), 26.2 (t), 28.7 (t), 29.1 (2×t), 29.2 (5×t), 29.4 (2×t), 30.0 (t), 31.6 (t), 34.2 (t), 50.1 (t), 58.0 (t), 64.2 (t), 67.5 (t), 69.5 (t), 75.0 (s), 75.4 (s), 77.4 (s), 78.7 (d), 122.5 (d), 143.1 ppm (s); IR (neat): $\tilde{\nu}_{max}$=3308, 2926, 2586, 2102, 1736 cm^{-1}; MS (ESI+): m/z: 562 $[M+H]^+$; elemental analysis calcd (%) for $C_{27}H_{55}B_{10}N_3O_2$: C 57.72, H 9.87, N 7.48; found: C 57.75, H 9.99, N 7.47.

o-*Carborane* ***9***: Method A: *o*-Carborane **8** (0.18 mmol, 0.10 g) and *tert*-butyl-DOTAMA-C_6 azide **15** (0.18 mmol, 0.12 g) in a 25 mL round-bottomed flask were suspended in H_2O/MeOH (4 mL, 50:50) solution with Cu−SILC (150 mg) and stirred at 60°C overnight under Ar. The solution was then filtered and the solvent was evaporated. The crude was purified by column chromatography (eluent: gradient from CH_2Cl_2/MeOH 98:2 to CH_2Cl_2/MeOH 80:20) to afford a pale yellow oil (0.04 g, 18%). Method B: *o*-Carborane **8** (0.33 mmol, 0.18 g) and *tert*-butyl-DOTAMA-C_6 azide **15** (0.33 mmol, 0.23 g) in a 50 mL round-bottomed flask were dissolved in H_2O/THF (10 mL, 50:50) and stirred overnight at RT in the presence of 20 mol% $Cu(OAc)_2$ (0.007 mmol, 0.30 g) and 40 mol% Na ascorbate (0.13 mmol, 0.03 g). The THF was then evaporated and CH_2Cl_2 was added. The aqueous phase was then extracted twice with CH_2Cl_2 and the organic phases were washed with brine (2×10 mL). The crude was purified by column chromatography (eluent: gradient from CH_2Cl_2/MeOH 98:2 to CH_2Cl_2/MeOH 80:20) to afford a pale yellow oil (0.15 g, 35%). ^1H NMR (200 MHz, $CDCl_3$, Me_4Si): δ=0.87 (brt, J=6.8 Hz, 3H; CH_3), 1.24 (brs, 26H; $CH_3(CH_2)_{13}$), 1.45 (s, 27H; *t*Bu), 1.50–1.70 (m, 8H; $CONHCH_2(CH_2)_4$, 1.89 (m, 2H; $CH_3(CH_2)_{13}CH_2$), 2.10–3.00 (m, 18H; NCH_2CH_2N, $B_{10}H_{10}C_2CH_2CH_2$), 3.10–3.40 (m, 10H; $NCH_2COOtBu$, $NHCH_2CH_2$), 3.59 (m, 2H; $B_{10}H_{10}C_2CH_2CH_2O$), 4.05 (s, 2H; $B_{10}H_{10}C_2CH_2O$), 4.27 (m, 4H; $N_3C_2CH_2O$), 4.65 (m, 4H; $CH_2N_3C_2$), 7.60 (m, 1H; HN_3C_2), 7.70 (m, 1H; HN_3C_2); 8.00 ppm (m, 1H; NH); ^{13}C NMR (50.2 MHz, $CDCl_3$, Me_4Si): δ=13.9 (q), 22.5 (t), 25.6 (t), 25.8 (t), 26.0 (t), 26.3 (t), 26.4 (t), 27.7 (9×q), 28.5 (t), 29.1 (t), 29.5 (9×t), 32.1 (t), 38.9 (t), 44.9 (t), 50.0–60.0 (14×t), 64.0 (t), 64.4 (t), 68.0 (t), 69.7 (t), 75.5 (s), 80.7 (s), 81.5 (2×s), 81.6 (s), 122.3 (d), 123.0 (d), 143.2 (s), 143.7 (s), 171.6 (s), 171.3 (s), 171.8 (s), 172.1 ppm (s); IR (neat): $\tilde{\nu}_{max}$=3420, 2927, 2574, 1732, 1674, 1539 cm^{-1}; MS (ESI+): m/z: 1260 $[M+H]^+$; elemental analysis calcd (%) for $C_{61}H_{119}B_{10}N_{11}O_9$: C 58.20, H 9.53, N 12.24; found: C 58.22, H 9.52, N 12.25.

Gd^{III}–MEA01: The ligand was dissolved in water at low concentration (0.1 mM) and the pH was adjusted to 7 by adding 1 M NaOH. An equimolar amount of $GdCl_3{\cdot}6H_2O$ was dissolved in water (0.5 mL) and slowly added to the first solution while maintaining the pH value at 6.5 with NaOH. The mixture was then stirred at room temperature for 16 h. Xylenol Orange UV spectrophotometry was used to check for the absence of free Gd^{III} ions.

Preparation of LDL adducts: MEA01 micelle disaggregation was carried out by mixing an excess amount of β-CD with a 0.07 mM complex solution (30′, 20°C, 50:1). MEA01-loaded LDL particles were prepared by incubating LDL (0.2 μM; Biomedical Technologies Inc., Stoughton, MA, USA) and MEA01/β-CD adducts (0.07 mM) for 2 h at 37°C. The β-CD and the unbound complex were eliminated by dialysis. MEA01-LDL loaded with 295 complexes per LDL particle was used for cell experiments. The final Gd concentration was determined by T_1 measurements in the ^1H NMR spectra of the mineralised complex solution (at 20 MHz, 258°C, in 6 M HCl at 120°C for 16 h) and the protein concentration was determined by means of a commercial Bradford assay (Biorad, Hercules, CA, USA).

Cell lines: Mouse melanoma (B16-F10) were obtained from the American Type Culture Corporation and the cells were cultured in Dulbecco's modified eagle medium (DMEM; Lonza) supplemented with glucose (4.5 gL^{-1}), 10% (v/v) fetal bovine serum (FBS), 2 mM glutamine, 100 U mL^{-1} penicillin, and 100 U mL^{-1} streptomycin. For uptake experiments, 3×10^5 B16 were seeded in 6 cm dishes. The cells were incubated the following day for 24 h with culture media added with 6% lipoprotein-deficient serum (Biomedical Technologies Inc., Stoughton, MA, USA) to increase low-density lipoprotein receptor (LDLR) expression. Finally, the cells were incubated for 16 h with MEA01-loaded LDL particles at different concentrations (10–50 μg mL^{-}1). At the end of the incubation, the cells were washed with ice-cold PBS (3×10 mL), detached with trypsin/ethylenediaminetetraacetic acid (EDTA), and transferred into glass capillaries for MRI analysis (see below). The B and Gd content in each cell line was determined by using inductively coupled plasma mass spectrometry (element-2; Thermo-Finnigan, Rodano (MI), Italy).

Magnetic resonance imaging: MR images were acquired using a Bruker Avance 300 spectrometer (7 T) equipped with a Micro 2.5 microimaging probe (Bruker BioSpin, Ettlingen, Germany). Glass capillaries that contained about 2×10^6 cells were placed in an agar phantom and MR imaging was performed by using a standard T_1-weighted multislice spin–echo sequence (TR/TE/NEX=200:3.3:8, FOV=1.2 cm, NEX=number of exitations; FOV=field of view). The T_1 relaxation times were calculated by using a standard saturation recovery spin echo.

Acknowledgements

The authors gratefully acknowledge financial and scientific support from Regione Piemonte, Nano-IGT project (Converging Technologies), ENCITE project (FP7-HEALTH-2007A), Fondazione Compagnia di San Paolo (Torino), and EU Action COST D38.

[1] R. F. Barth, *J. Neuro-Oncol.* **2003**, *62*, 1.

[2] R. F. Barth, J. A. Coderre, M. G. H. Vicente, T. E. Blue, *Clin. Cancer Res.* **2005**, *11*, 3987.
[3] M. F. Hawthorne, M. W. Lee, *J. Neuro-Oncol.* **2003**, *62*, 33.
[4] A. H. Soloway, W. Tjarks, B. A. Barnum, F. G. Rong, R. F. Barth, I. M. Codogni, J. G. Wilson, *Chem. Rev.* **1998**, *98*, 1515.
[5] J. F. Valliant, K. J. Guenther, A. S. King, P. Morel, P. Schaffer, O. O. Sogbein, K. A. Stephenson, *Coord. Chem. Rev.* **2002**, *232*, 173.
[6] G. Wu, R. F. Barth, W. Yang, R. J. Lee, W. Tjarks, M. V. Backer, J. M. Backer, *Anti-Cancer Agents Med. Chem.* **2006**, *6*, 167.
[7] E. L. Crossley, E. J. Ziolkowski, J. A. Coderre, L. M. Rendina, *Mini-Rev. Med. Chem.* **2007**, *7*, 303.
[8] H. C. Kolb, M. G. Finn, K. B. Sharpless, *Angew. Chem. Int. Ed.* **2001**, *40*, 2004.
[9] H. C. Kolb, K. B. Sharpless, *Drug Discovery Today* **2003**, *8*, 1128.
[10] C. R. Becer, R. Hoogenboom, U. S. Schubert, *Angew. Chem. Int. Ed.* **2009**, *48*, 4900.
[11] J.-F. Lutz, *Angew. Chem. Int. Ed.* **2008**, *47*, 2182.
[12] S. Aime, A. Barge, A. Crivello, A. Deagostino, R. Gobetto, C. Nervi, C. Prandi, A. Toppino, P. Venturello, *Org. Biomol. Chem.* **2008**, *6*, 4460.
[13] S. Geninatti-Crich, D. Alberti, I. Szabo, A. Deagostino, A. Toppino, A. Barge, F. Ballarini, S. Bortolussi, P. Bruschi, N. Protti, S. Stella, S. Altieri, P. Venturello, S. Aime, *Chem. Eur. J.* **2011**, *17*, 8479.
[14] J. C. Jewett, C. R. Bertozzi, *Chem. Soc. Rev.* **2010**, *39*, 1272.
[15] J. M. Bryson, W. J. Chu, J. H. Lee, T. M. Reineke, *Bioconjugate Chem.* **2008**, *19*, 1505.
[16] S. Knör, A. Modlinger, T. Poethko, M. Schottelius, H.-J. Wester, H. Kessler, *Chem. Eur. J.* **2007**, *13*, 6082.
[17] I. Dijkgraaf, A. Y. Rijnders, A. Soede, A. C. Dechesne, G. W. van Esse, A. J. Brouwer, F. H. M. Corstens, O. C. Boerman, D. T. S. Rijkers, R. M. J. Liskamp, *Org. Biomol. Chem.* **2007**, *5*, 935.
[18] Y. Song, E. K. Kohlmeir, T. J. Meade, *J. Am. Chem. Soc.* **2008**, *130*, 6662.
[19] C.-B. Yim, O. C. Boerman, M. de Visser, M. de Jong, A. C. Dechesne, D. T. S. Rijkers, R. M. J. Liskamp, *Bioconjugate Chem.* **2009**, *20*, 1323.
[20] C. B. Yim, I. Dijkgraaf, R. Merkx, C. Versluis, A. Eek, G. E. Mulder, D. T. S. Rijkers, O. C. Boerman, R. M. J. Liskamp, *J. Med. Chem.* **2010**, *53*, 3944.
[21] M. Q. Tan, X. M. Wu, E. K. Jeong, Q. J. Chen, Z. R. Lu, *Biomacromolecules* **2010**, *11*, 754.
[22] A. E. Martell, R. D. Hancock, *Metal Complexes in Aqueous Solution*, Plenum Press, New York, **1996**.
[23] W. P. Cacheris, S. K. Nickle, A. D. Sherry, *Inorg. Chem.* **1987**, *26*, 958.
[24] R. E. Mewis, S. J. Archibald, *Coord. Chem. Rev.* **2010**, *254*, 1686.
[25] M. K. Schultz, S. G. Parameswarappa, F. C. Pigge, *Org. Lett.* **2010**, *12*, 2398.
[26] M. E. Martin, S. G. Parameswarappa, M. S. O'Dorisio, F. C. Pigge, M. K. Schultz, *Bioorg. Med. Chem. Lett.* **2010**, *20*, 4805.
[27] T. Katayama, K. Kamata, K. Yamaguchi, N. Mizuno, *Chemsuschem* **2009**, *2*, 59.
[28] K. Yamaguchi, T. Oishi, T. Katayama, N. Mizuno, *Chem. Eur. J.* **2009**, *15*, 10464.
[29] C. Girard, E. Onen, M. Aufort, S. Beauviere, E. Samson, J. Herscovici, *Org. Lett.* **2006**, *8*, 1689.
[30] U. Sirion, Y. J. Bae, B. S. Lee, D. Y. Chi, *Synlett* **2008**, 2326.
[31] H. Hagiwara, H. Sasaki, T. Hoshi, T. Suzuki, *Synlett* **2009**, 643.
[32] C. Di Meo, L. Panza, F. Campo, D. Capitani, L. Mannina, A. Banzato, M. Rondina, A. Rosato, V. Crescenzi, *Macromol. Biosci.* **2008**, *8*, 670.
[33] B. A. Wojtczak, A. Andrysiak, B. Gruner, Z. J. Lesnikowski, *Chem. Eur. J.* **2008**, *14*, 10675.
[34] Z. J. Lesnikowski, *J. Organomet. Chem.* **2009**, 694, 1771.
[35] R. Djeda, J. Ruiz, D. Astruc, R. Satapathy, B. P. Dash, N. S. Hosmane, *Inorg. Chem.* **2010**, *49*, 10702.
[36] Y. Wu, P. J. Carroll, W. Quintana, *Polyhedron* **1998**, *17*, 3391.
[37] R. W. Berg, M. Deetlef, K. R. Seddon, I. Shim, J. M. Thompson, *J. Phys. Chem. B* **2005**, *109*, 19018.
[38] A. Barge, L. Tei, D. Upadhyaya, F. Fedeli, L. Beltrami, R. Stefania, S. Aime, G. Cravotto, *Org. Biomol. Chem.* **2008**, *6*, 1176.
[39] K. C. Briley-Saebo, S. Geninatti-Crich, D. P. Cormode, A. Barazza, W. J. M. Mulder, W. Chen, G. B. Giovenzana, E. A. Fisher, S. Aime, Z. A. Fayad, *The Journal of Physical Chemistry B* **2009**, *113*, 6283.
[40] S. Geninatti-Crich, D. Alberti, I. Szabo, A. Deagostino, A. Toppino, A. Barge, F. Ballarini, S. Bortolussi, P. Bruschi, N. Protti, S. Stella, S. Altieri, P. Venturello, S. Aime, *Chem. Eur. J.* **2011**, *17*, 8479.

Received: May 9, 2012
Revised: September 14, 2012
Published online: November 14, 2012

